Dalton Transactions

Weakly Interacting Solvation Spheres Surrounding a Calixarene-Protected Tetrairidium Carbonyl Cluster: Contrasting Effects on Reactivity of Alkane Solvent and Silica Support

Journal:	*Dalton Transactions*
Manuscript ID	DT-ART-04-2018-001371.R2
Article Type:	Paper
Date Submitted by the Author:	21-Aug-2018
Complete List of Authors:	Palermo, Andrew; University of California Davis, Chemical Engineering Zhang, Shengjie; The University of Alabama, Chemistry Hwang, Sonjong; California Institute of Technology, Chemistry and Chemical Engineering Dixon, David; University of Alabama, Chemistry Gates, Bruce; University of California, Department of Chemical Engineering Katz, Alexander; UC Berkeley, Chemical Engineering

Journal

ARTICLE

Weakly Interacting Solvation Spheres Surrounding a Calixarene-Protected Tetrairidium Carbonyl Cluster: Contrasting Effects on Reactivity of Alkane Solvent and Silica Support

67Received 00th January 20xx,
Accepted 00th January 20xx

DOI: 10.1039/x0xx00000x

www.rsc.org/

Andrew P. Palermo[a,b], Shengjie Zhang[c], Son-Jong Hwang[d], David A Dixon[c]*, Bruce C. Gates[a]*, Alexander Katz[b]*

Abstract: The tetrairidium carbonyl cluster $Ir_4L_3(CO)_9$ (L = *tert*-butyl-calix[4]arene$(OPr)_3(OCH_2PPh_2)$ (Ph = phenyl; Pr = propyl)) on a partially dehydroxylated silica support undergoes hydrogen activation at a rate and with a mechanism different from those pertaining to the cluster in alkane solution. These results are unobvious in view of the sterically bulky ligands protecting the cluster and the nearly identical CO band frequencies in the infrared spectra characterizing the supported and dissolved $Ir_4L_3(CO)_9$, both before reaction and during reaction involving decarbonylation in the presence of either helium or H_2 (and H_2 reacted with the clusters to form hydrides with the same Ir-H band frequencies for clusters in alkane solvent and supported on silica). The initial rates of CO loss from the supported clusters in the presence of helium were the same as those in the presence of H_2. The comparison demonstrates that the rate-determining step for hydride formation on the silica-supported cluster is CO dissociation. In contrast, the comparable dissociation of CO from the cluster in *n*-decane solution requires a higher temperature, 343 K, and is at least an order of magnitude slower than when the clusters were supported on silica. CO dissociation is not the rate-determining step for hydrogen activation on the cluster in *n*-decane, as the rate is influenced by reactant H_2 as well.

Introduction

In contrast to metal complexes in inert solutions, metal complexes immobilized on solids are often perturbed by interactions with surface functional groups (e.g., Lewis-acidic cations)[1,2] or distortion brought about by steric influences of narrow internal pores of the support (e.g., zeolite cavities).[3] Yet there are only a limited number of cases in which the metal complex is nearly identical in the soluble and surface-anchored states, as characterized by infrared (IR) spectroscopy of CO ligands on the metal (save for minor isotropic band broadening) as IR spectroscopy is among the most sensitive of characterization techniques for assessing structural differences of metal carbonyl complexes.[1,3] In these cases, an unresolved issue is whether rate processes are also identical for the soluble and supported metal complexes.

Herein we report results for the reactions of substituted tetrairidium clusters, consisting of the previously described and fully characterized cluster $Ir_4L_3(CO)_9$ (L = *tert*-butyl-calix[4]arene$(OPr)_3(OCH_2PPh_2)$ (Pr = propyl; Ph = phenyl), shown in Scheme 1.[2,5,6] The bulky calixarene ligands act as spacers that not only separate clusters from each other, disfavoring aggregation,[2,5–7] but also separating the metal cores from the support surface. The unsubstituted variant of this cluster, Ir_4CO_{12}, has been previously shown to have nearly identical IR spectra in organic solution and when supported on silica.[4] We investigated a simple rate process involving dissociation of CO from the clusters in the presence of inert helium and, for comparison, in the presence of reactive hydrogen, with the goal of determining the effect of cluster environment on rate, specifically comparing the rates of CO loss from the clusters on silica and in alkane solvent.

Results

Soluble and supported $Ir_4L_3(CO)_9$ was characterized with IR and ^{31}P NMR spectroscopies. Figure 1 shows IR spectra of the supported clusters and the clusters in *n*-decane solution. Both spectra include bands at the same frequencies for terminal (2043 and 1994 cm^{-1}) and bridging (1787 cm^{-1}) CO ligands.[8] The integration of the solution-phase ^{31}P and solid-state ^{31}P CP/MAS NMR spectra (Figures S1 and S2 in the ESI) demonstrates the same ratio of two equatorial to one axial phosphine ligand (corresponding to resonances at 19.29 and -13.12 ppm, respectively[8]).

[a] Department of Chemical Engineering
University of California, Davis, Davis, CA 95616 (USA).
E-mail: bcgates@ucdavis.edu
[b] Department of Chemical and Biomolecular Engineering
University of California, Berkeley, Berkeley, California 94720 (USA).
E-mail: askatz@berkeley.edu
[c] Department of Chemistry, The University of Alabama, Tuscaloosa, Alabama 35487, (USA)
Email: dadixon@ua.edu
[d] Division of Chemistry and Chemical Engineering
California Institute of Technology, Pasadena, California 91125 (USA)

† Electronic Supplementary Information (ESI) available: Additional infrared spectra, ^{31}P nuclear magnetic spectra, kinetics data, and mass spectrometry; see DOI: 10.1039/x0xx00000x

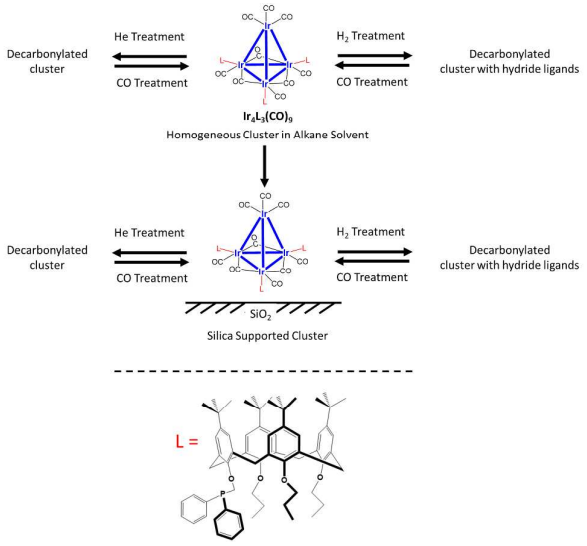

Scheme 1. Schematic representation of homogeneous and silica-supported tetrairidium clusters $Ir_4L_3(CO)_9$ and their reactions when exposed to helium, H_2, and CO. The CO loss occurred at the basal plane where calixarene phosphine ligands (L) are located.[9] For clarity, the silica surface is represented as flat, although in reality, on the length scale of the cluster, it is likely roughened. See text and Electronic Supporting Information (ESI) for details.

Starting from $Ir_4L_3(CO)_9$ dissolved in anhydrous *n*-decane, we attempted to dissociate CO from the cluster by bubbling helium through the solution. At 323 K (Figure 2a), there was no detectable decarbonylation, and at 343 K there was only slight decarbonylation (<4% of the CO removed) over 24 h. Using the ν_{CO} band areas determined during the decarbonylation at 343 K (details in the Experimental Methods section), we determined the initial rate of CO dissociation to be 5.1×10^{-3} and 9.1×10^{-3} (mol of CO removed)/(mol of Ir_4 cluster × h) for the terminal and bridging CO ligands, respectively (Table 1). Following this

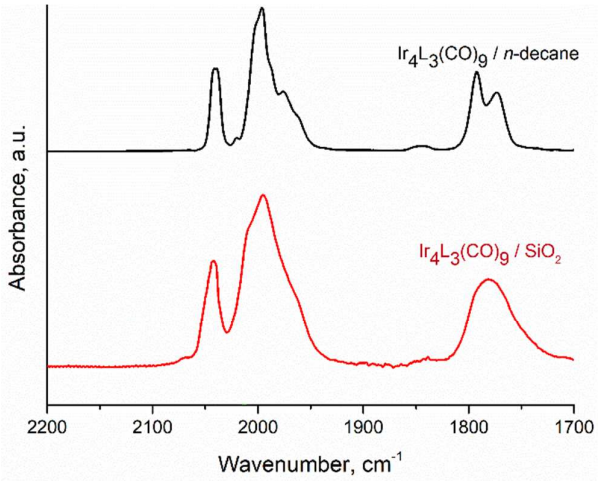

Figure 1. IR carbonyl spectra of $Ir_4L_3(CO)_9$ clusters dissolved in distilled *n*-decane and solid-state IR spectra of supported $Ir_4L_3(CO)_9$ clusters on dehydroxylated SiO_2. The IR spectra of Figure 1 provide a comparison of these clusters in the two states on the basis of the carbonyl stretching frequencies, which are a sensitive measure of the environment as these frequencies are essentially identical (Table 1 and Figure S3 in the ESI).

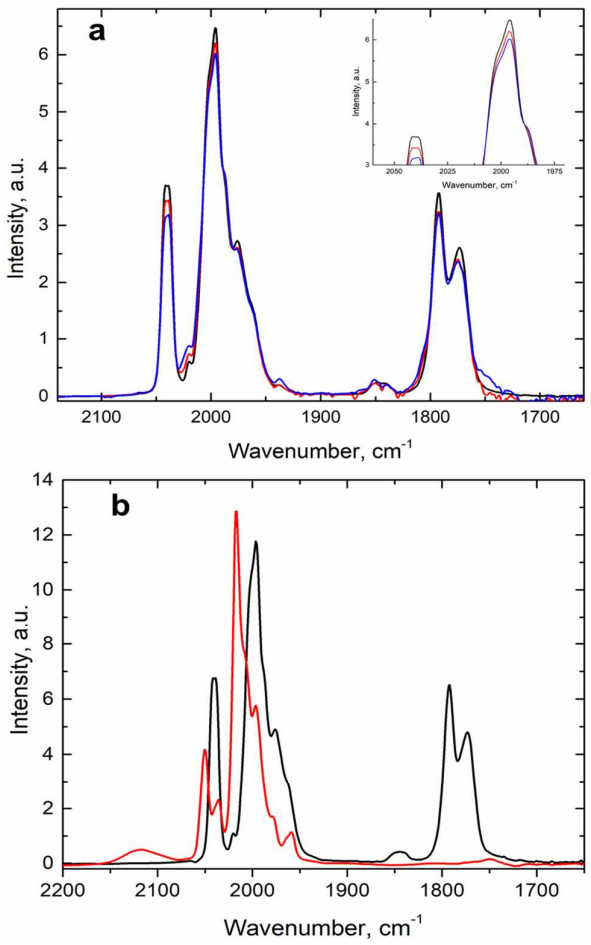

Figure 2. (a) Solution IR spectra in the ν_{CO} region characterizing $Ir_4L_3(CO)_9$ in anhydrous *n*-decane during exposure to helium at room temperature (black), followed by 24 h at 343 K (red), and an additional 24 h at 353 K (blue). (b) Solution IR spectra in ν_{IrH} and ν_{CO} region characterizing $Ir_4L_3(CO)_9$ in anhydrous *n*-decane at 1 bar and 333 K before (black) and after (red) exposure to H_2.

treatment, we attempted further decarbonylation at the higher temperature of 353 K (Figure 2a), but only 0.24 terminal and 0.23 bridging carbonyl ligands had been removed per cluster after 24 h, evidently just by thermal dissociation.

We also carried out experiments with $Ir_4L_3(CO)_9$ in *n*-decane under reactive conditions, as H_2 was bubbled through the solution. The IR spectra show that significant CO loss occurred at temperatures as low as 333 K after 24 h (although no measurable CO loss was observed after 24 h at 323 K), with one terminal and all bridging carbonyl ligands removed per cluster (Figure 2b). The initial rates were found from the band areas to be 4.2×10^{-2} and 1.3×10^{-1} (mol of CO removed)/(mol of Ir_4 cluster × h) for terminal and bridging carbonyls, respectively. These rates are an order of magnitude higher than those reported above for the sample exposed to flowing helium. As a result of the reaction of the clusters with H_2 at 333 K for 24 h, there were changes in the ν_{CO} bands shown in Figure 2b: five bands were blue-shifted, from 2041, 2020, 1995, 1987, and 1976 cm^{-1} to 2050, 2035, 2016, 2007, and 1996 cm^{-1}, respectively. Concomitantly, an Ir–H band appeared, at 2110 cm^{-1} (Figure 2b). The CO band shifts are

associated with the presence of the neighboring hydride ligands on the clusters. These changes are contrasted with the much more complex changes in the IR spectra that accompany the breaking of cluster Ir–Ir bonds during reactions with H_2,[10,11] which cannot be described by a simple blue-shift translation of existing bands and instead indicate the appearance of new bands forming while others disappeared. We thus rule out the possibility of breakup of the cluster frame during the reaction with H_2.

To compare the reactivity of the silica-supported clusters with those in solution, we investigated the rate of CO dissociation of the supported clusters while again recording IR spectra with the sample in contact with flowing helium (Figure 3a) and with flowing H_2 (Figure 3b).[12] In the presence of helium, both terminal and bridging carbonyl ligands were lost from the clusters (Figure S4 and S5, SI), with a ratio of bridging to terminal carbonyl removal of approximately 2:1 throughout the process (Figure S5b, ESI—the initial value of the bridging CO to terminal CO ligand ratio in the cluster was 1:3).[13] The rate of decarbonylation declined as the process proceeded (Figure 3c). Using the integrated band areas of the terminal CO bands initially at 2043 and 1994 cm^{-1} (Figure S5, ESI) and of the bridging carbonyl band initially at 1787 cm^{-1} (Figure S5, ESI) we determined the initial decarbonylation rates at 323 K to be 4.20 ± 0.01 × 10^{-2} and 1.09 ± 0.04 × 10^{-1} (mol of CO removed)/(mol of Ir_4 cluster × h), respectively (Table 1, Figure S6, ESI), with the former value being based on data for the two terminal CO bands, each of which gave the same results within experimental uncertainty (details in ESI). After 40 h in helium at 323 K, these bands had decreased in intensity until decarbonylation ceased (Figure 3a and S5 in ESI). The band areas imply that 0.5 of the original six terminal carbonyl ligands and one of the original three bridging carbonyl ligands had been removed per cluster (Figure S7, ESI). We subsequently exposed the partially decarbonylated supported clusters to CO flowing at 1 bar and 323 K, and the spectra show that the decarbonylation was rapid and almost fully reversed, with 99% of the initial terminal band intensity and 96% of the initial bridging band intensity being recovered within 10 h (Figure 3c).

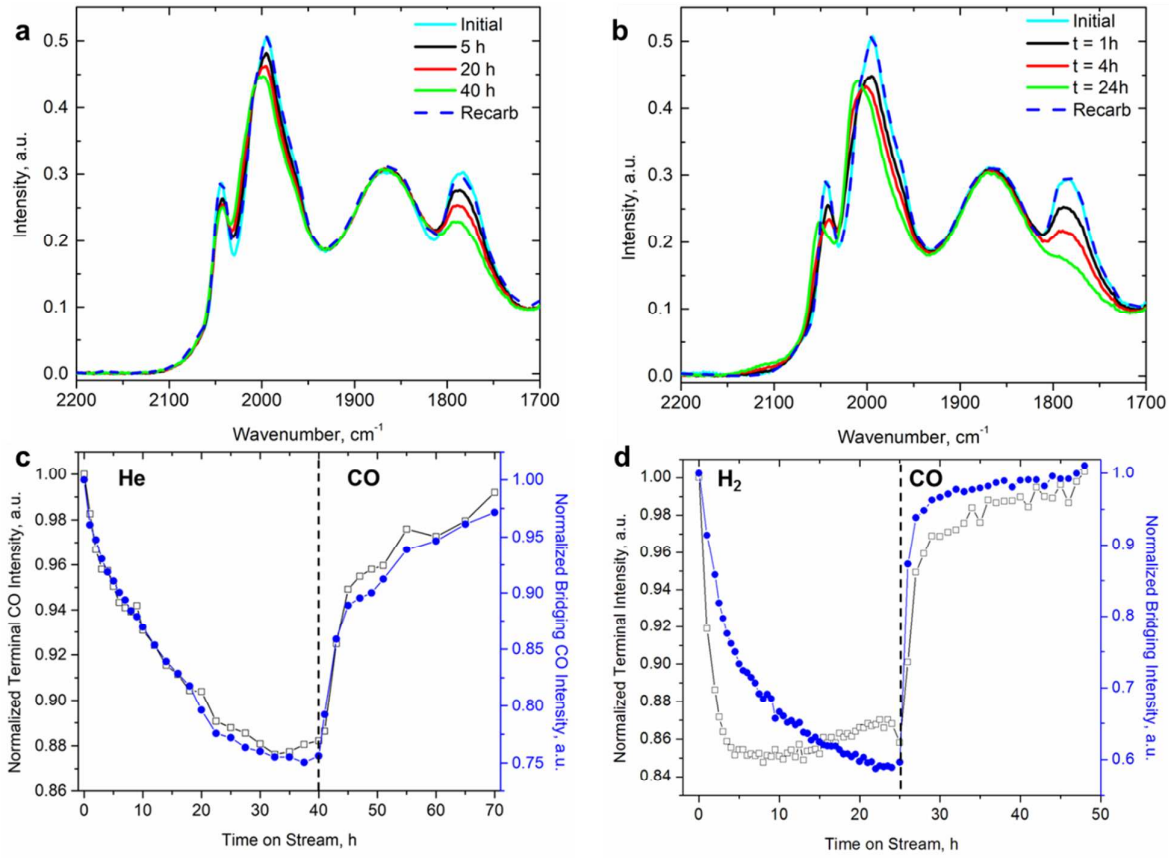

Figure 3. IR spectra of silica-supported $Ir_4L_3(CO)_9$ in the carbonyl stretching region undergoing decarbonylation in the presence of flowing (a) helium and (b) H_2 at 323 K and 1 bar. The intensity of the terminal carbonyl band initially at 1994 cm^{-1} and that of the bridging carbonyl band at 1787 cm^{-1} are represented as a function of time on stream in (c) and (d) for the helium and H_2 treatments, respectively. After the sample had reached a steady state under each set of treatment conditions (shown by dashed vertical lines in (c) and (d)), a subsequent treatment in flowing CO was carried out at 323 K and 1 bar, leading to cluster recarbonylation. The black squares in (c) and (d) represent the terminal CO intensity, and blue circles represent the bridging CO intensity.

Table 1. Initial decarbonyation rates of $Ir_4L_3(CO)_9$ clusters in anhydrous *n*-decane and adsorbed on dehydroxylated SiO_2

Type of ligand removed/solvent or support	Temperature of decarbonylation in He (K)	Rate of decarbonylation in He (mol of CO removed)/ (mol of Ir_4 cluster × h)	Temperature of decarbonylation in H_2 (K)	Rate of decarbonylation in H_2 (mol of CO removed)/ (mol of Ir_4 cluster × h)	Carbonyl Band Frequencies Used in Figure S3[a]
Terminal CO/ SiO_2	**323**	$(4.20 \pm 0.01) \times 10^{-2}$	**323**	$(4.19 \pm 0.02) \times 10^{-2}$	2043, 2003, 1994, 1964
Bridging CO/ SiO_2	**323**	$(1.09 \pm 0.04) \times 10^{-1}$	**323**	$(1.21 \pm 0.01) \times 10^{-1}$	1782
Terminal CO/ *n*-decane	**343**	$(5.1 \pm 0.01) \times 10^{-3}$	**333**	$(4.2 \pm 0.02) \times 10^{-2}$	2041, 2005, 1995, 1962
Bridging CO/ *n*-decane	**343**	$(9.1 \pm 0.33) \times 10^{-3}$	**333**	$(1.3 \pm 0.01) \times 10^{-1}$	1791[b], 1774[b]

[a]The most prominent bands and shoulders were selected from the spectra in Figure 1 prior to any decarbonylation.

[b]The bridging carbonyl band at 1782 cm^{-1} characterizing the cluster on silica is the average of the bands characterizing the cluster in solution, at 1791 and 1774 cm^{-1}.

After extended reaction with the samples in flowing H_2, both the $Ir_4L_3(CO)_9$ clusters dissolved in *n*-decane and those supported on silica underwent removal of one terminal and two bridging carbonyl ligands from each cluster (Figures 3b, 3d, and S8, ESI). The final spectra following reaction with H_2 are shown in Figure 4; they indicate the same wavelengths of the terminal CO bands, independent of whether the clusters were in solution or supported on silica. A slight difference between the two spectra is evident: a very weak bridging CO band was still observed for the silica-supported cluster but not for the dissolved cluster, a difference that we attribute to the 10 K higher decarbonylation temperature applied to the solution (full removal of bridging carbonyls has been observed at higher temperatures for the silica-supported sample in the presence of flowing H_2)[9].

Below we analyze the kinetics of the growing hydride band and the declining terminal and bridging carbonyl bands observed during the reaction of the silica-supported $Ir_4L_3(CO)_9$ cluster in H_2; these data are shown in Figure 5a (normalized such that an intensity of 1 corresponds to the maximum band area and zero represents the minimum. Note that zero does not mean the lack of absorbance in Figure 5a). The two terminal CO ligands disappeared at the same rate, within experimental uncertainty (Figures S9, 10a, and 10b and Table S1 in the ESI; details in ESI), but the hydride band growth and bridging carbonyl band loss took place at rates different from those of the loss of the two terminal CO ligands (Figures 3, S9a, and S9b, and Table S1 in the ESI, details in ESI). The ratio of bridging to terminal carbonyl ligand loss of 2 (Figure S5 and S9 in the ESI) was the same in the presence of H_2, as in the presence of helium. At 323 K, the loss of terminal CO from the silica-supported cluster is characterized by an initial rate of $(4.19 \pm 0.02) \times 10^{-2}$ (mol of CO removed)/(mol of Ir_4 cluster × h) and that of the bridging band, initially at 1776 cm^{-1}, by an initial rate of $(1.21 \pm 0.01) \times 10^{-1}$ (mol of CO removed)/(mol of Ir_4 cluster × h) (Table 1). These initial rates match, within experimental uncertainty, values observed for CO dissociation on the same supported clusters exposed to helium instead of H_2 at the same temperature.

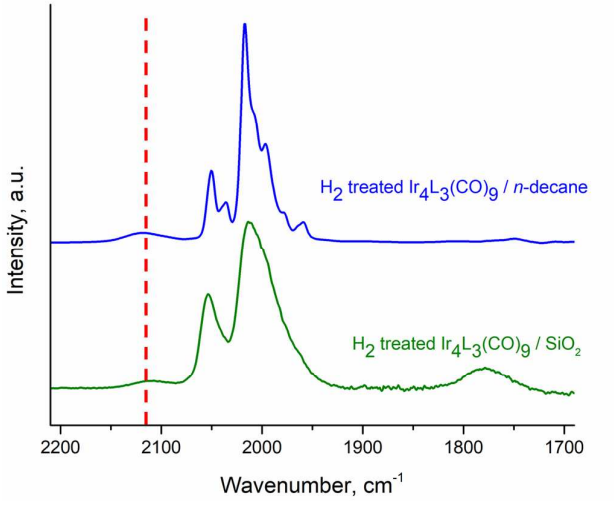

Figure 4. Carbonyl IR spectra of $Ir_4L_3(CO)_9$ clusters in *n*-decane (blue) and supported on dehydroxylated SiO_2 (green). The former data were recorded after H_2 bubbled through the solution at 333 K for 24 h and the latter after H_2 flowed through the sample at 323 K for 24 h. The red line is shown to demonstrate an overlay of hydride band assignment between the clusters in solution (blue) and on silica.

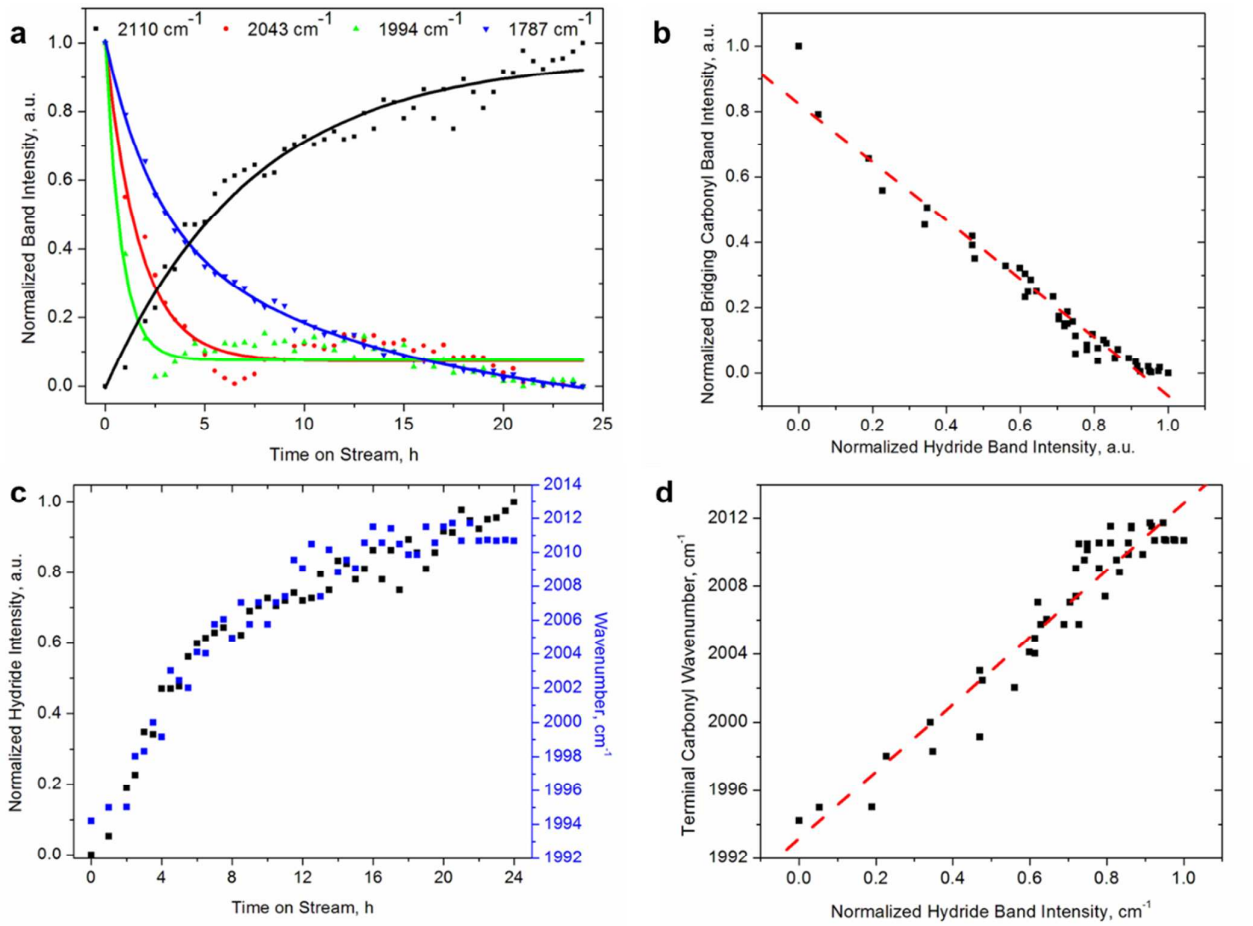

Figure 5. (a) Normalized band intensities of carbonyl and hydride species on the tetrairidium clusters during reaction in H_2. (b) Correlation of growth of the Ir–H band at 2110 cm^{-1} with the frequency of the terminal CO band. (c) Normalized hydride band intensity (black) and terminal carbonyl wavenumber (blue) recorded during the reaction with H_2. (d) Terminal carbonyl correlated with the normalized hydride band intensity (sample in flowing mixture of H_2, 10 mL/min, and helium, 50 mL/min; temperature = 323 K, pressure = 1.0 bar; sample mass = 30 mg; iridium loading = 1 wt.%)

We emphasize that even though the reported decarbonylation rates of the supported clusters in flowing H_2 are almost the same as those of the clusters in *n*-decane solution reported in Table 1, these two experiments were performed at different temperatures. CO dissociation rates in the presence of helium were at least a factor of 10 higher for the silica-supported clusters than those dissolved in *n*-decane.

The data of Figure 3b show that the bonding of hydride ligands to the clusters on silica is reversible: the appearance of the hydride band at 2110 cm^{-1} and the blue shift that accompanied it as H_2 reacted with the supported $Ir_4L_3(CO)_9$ were completely reversed when the sample was brought in contact with flowing CO. Thus, the spectrum (dashed line in Figure 3b) observed after CO dissociation with the sample in H_2 followed by recarbonylation is indistinguishable from that of the initially supported $Ir_4L_3(CO)_9$. These results confirm that the cluster frame remained fully intact during the changes in the cluster ligand sphere and that the bonding sites for CO were the same ones present initially.

Further characterization data are presented in the ESI, with a discussion regarding the removal of hydride ligands and identification of the off-gas as H_2 during recarbonylation (Figures S11 and S12).

To provide some further insight, we used electronic structure calculations at the level of density functional theory with the hybrid B3LYP exchange-correlation functional to model the properties including bond energies of $Ir_4(CO)_xL_y$ clusters with various phosphorus-containing ligands (see Tables S2 and S3 in the ESI).[14] We calculated the bond energies to remove CO from $Ir_4(CO)_9L_3$ clusters with L = $PMePh_2$, with the clusters in the gas phase and in aqueous and hexane solutions; we used an implicit self-consistent reaction field (SCRF) approach to model the solvent. The results, summarized in the ESI, show that there is essentially no effect (< 4 kJ/mol) of whether the CO is released from a gas-phase cluster or from a solvated cluster.

Discussion

Lack of Influence of Environment on Structure of $Ir_4L_3(CO)_9$ Cluster Assessed by Stretching Frequencies of Carbonyl Ligands

The observation that the CO band frequencies characterizing the $Ir_4L_3(CO)_9$ clusters (Figures 2 and 4, and Table 1) are independent of whether the clusters are in solution or on a support, during CO loss occurring in helium or H_2, implies that the effects on the cluster structure of the alkane solvent and the silica support are similar.[1,3] This result is in line with reports of essentially the same CO band frequencies of $Ir_4(CO)_{12}$ supported on silica, dissolved in dichloromethane, and present in the crystalline state with the frequency differences within 3 cm^{-1}.[15,16] A similar conclusion is drawn by comparing the same frequency of the Ir-H band for the cluster dissolved in alkane solvent and when silica supported, in Figure 4.

Lack of Transport Influence on Rates of Cluster Decarbonylation

The contrasting time scales for the decarbonylation and recarbonylation processes in the silica-supported clusters (Figures 3c and 3d) indicate that transport limitations were insignificant, both in the presence of helium and H_2.

Influence of Environment on Reactivity of $Ir_4L_3(CO)_9$ Clusters Indicated by Mechanism of H_2 Activation with Decarbonylation

Notwithstanding the lack of influence of the surroundings on the cluster structure, the initial rates of CO dissociation from the clusters in helium and in H_2 are markedly different for the dissolved and supported clusters. When the clusters were supported on silica, the rates of CO loss in H_2 and in helium were essentially the same. In contrast, when the clusters were present in *n*-decane solution, these rates were strikingly different in helium vs. H_2 (Figure 2). For instance, in H_2, four carbonyl ligands were removed per cluster at 333 K, whereas in helium essentially none were removed at 343 K.

These data indicate a H_2-dependent pathway for CO loss and hydrogen activation on $Ir_4L_3(CO)_9$ in *n*-decane, with CO dissociation not being rate determining. Associative mechanisms have been suggested for CO loss from substituted tetrairidium clusters (Sonnenberger and Atwood reported an associative mechanism for the reaction of $Ir_4(CO)_{11}(AsPh_3)$ with $AsPh_3$ in *n*-decane, whereas in chlorobenzene, CO loss from the same cluster proceeded via a dissociative mechanism[17]), so we infer that it is possible that loss of CO from our cluster in the presence of H_2 is also an associative process (but further investigations are needed to characterize this).

In contrast, because the data show that the rates of CO loss from the silica-supported $Ir_4L_3(CO)_9$ clusters are independent of whether H_2 is present, we infer that CO dissociation precedes H_2 activation and is rate-determining in the H_2 activation process (i.e., a vacant site is needed on the supported Ir cluster before H_2 activation can occur).

The data show that hydride ligands replaced both terminal and bridging carbonyls in the silica-supported clusters, as evidenced by the direct relationships between the intensities of the bands of the bridging (Figure 5b) and terminal (Figure S13, ESI) carbonyl ligands and that of the hydride ligands. Further, the data of Figure 5c and 5d demonstrate a direct relationship between the intensity of the growing hydride band and the blue shift of the terminal carbonyl band initially observed at 1994 cm^{-1}. Although a similar blue shift was reported in early work with compounds such as Vaska's complex;[18,19] our data appear to be the first to show both blue shifts of the carbonyl bands and the concomitant formation of metal hydride bands, a result that was facilitated by the opportunity afforded by our sample to simultaneously monitor both sets of bands. All the results are consistent with the inference that H_2 reacted with Ir centers in an oxidative addition leading to the replacement of CO ligands by hydrides.

The relationship between the blue shift of the terminal carbonyl band and the metal hydride band intensity (Figure 5d) indicates a high degree of uniformity of the Ir sites for bonding of hydrogen to the cluster frame—with each site contributing essentially equally to the terminal CO blue shift, regardless of the degree of cluster saturation with hydrogen. These results strongly support the choice of the tetrairidium clusters as nearly ideal samples to investigate for elucidation of the fundamental chemistry of H_2 activation at metal centers.

We infer that the possibility that the support interacts with the clusters via reverse spillover is unlikely, on the basis of the IR and NMR spectra shown in Figures 3 and S1 of the ESI, respectively. These two spectroscopic techniques are sensitive to environment and can detect the formation of hydrides, but none was observed. Had the hydrides formed, we would expect to have observed an Ir–H band and a carbonyl blue shift in the IR spectra during the treatment in helium or a shift in the P resonance in the ^{31}P NMR spectrum.

Role of the Support on Reactions on Ligated Iridium Clusters

It is important that although the difference in rates characterizing the dissolved and supported clusters was clearly observable under our experimental conditions, a difference of a factor of 10 in the rate at the temperatures of our experiments corresponds to an energy difference in the two processes of less than 6 kJ/mol. Such a small energy difference can arise from enthalpic and/or entropic contributions, and it is difficult to discern what energy terms control the rate. In the discussion that follows, we suggest various possibilities to account for these small energy differences.

One might postulate that in the treatment in helium, thermal dissociation of CO creates a vacancy on the Ir_4 frame and that the filling of this vacancy occurs by coordination of the silica support via lone electron pairs on bridging surface oxygen atoms. Such a mechanism would be similar to those hypothesized previously involving bridging oxygen atoms on inorganic oxide surfaces acting as Lewis bases, which coordinate to vacancy sites of anchored metal carbonyl complexes (and such reactions may often occur together with the coordination of support surface Lewis acid sites to CO ligands on the supported metal), but strong Lewis acid sites are absent from silica.[20] In contrast to this postulate, coordination by lone-pairs of oxygen atoms on silica would be expected to result in changes in the carbonyl IR spectra, that is, differences in the spectra characterizing the supported and dissolved samples after decarbonylation in helium (i.e., a red shift of CO bands for the silica-supported sample), unless the interaction of the O lone pairs were very similar electronically to that of the lone pair on C of CO interacting with the framework (cancelation of effects could be argued for $Ir_4(CO)_{12}$–for which the silica-supported and dichloromethane-dissolved clusters have nearly identical CO

frequencies[15]). If we were to accept the hypothesis that silica acting as a macroscopic ligand coordinates to CO vacancies on the Ir_4 core following decarbonylation in helium, we would infer that it must have involved some local rearrangement of the fairly rigid cone of the calixarene ligands on the cluster[12] to allow access to the metal core. We have separately investigated such conformational rearrangements in the more flexible calix[6]arene and calix[8]arene ligands bound to the surfaces of metal nanoparticles.[21,22] Similar rearrangements must also be occurring during the controlled assembly of Au_{11}-sized clusters comprising cone calix[4]arene ligands, during synthesis of nanoporous gold with Au-Au connectivity and intact calixarene surface ligands, after treatment of the clusters under forcing electrochemical reducing conditions.[23] The rigid cone calix[4]arene ligands in this case prevent the uncontrolled dendritic aggregation of the Au cores that would ensue under these conditions, and instead enable hydrogen-bubble templating of nanoscale pores.[23] The magnitude of the electronic support effect in such a case would be expected to be comparable to those demonstrated by coordinating furanic solvents catalyzing reactions on metal carbonyl complexes whereby coordination occurs through the oxygen lone pairs of the solvent to the vacancy as it forms.[24]

On the basis of the calculated bond energies for CO removal from $Ir_4(CO)_9L_3$ with L = $PMePh_2$ determined using an implicit SCRF model, we infer that the lack of an observed solvent effect on the thermodynamics of the CO dissociation energy is not surprising given that the cluster with three phosphine ligands is so large, with the size and electronic properties essentially unaffected by the loss of one CO molecule. Thus, the free energies of solvation of the parent cluster and of the cluster formed by loss of a CO ligand are closely comparable to each other. Furthermore, the free energy of solvation of CO is very small, so that it barely matters whether it is solvated or not. We infer that the comparison extends to the supported cluster in the gas phase vs. one in solution, discounting the effect of long-range interactions involving silica as a "solvent."

An alternative explanation is that there could be a dynamic effect whereby the release of CO is more effectively blocked by the surrounding calixarene ligands which have to do more work to open up to allow the CO to depart from the calixarene surrounded by solvent molecules than from the cluster on the silica surface. This possibility would involve the formation of a molecular channel between calixarenes when anchored on silica, associated with interactions between the calixarene ligands and the silica surface, which could enable the CO to leave more readily through this channel. The behavior in solution is what is often observed in many protein systems whereby an arm of the protein controls access to the active site to control the rate of an enzymatic reaction.[25] Again, if such an arm were held open in the cluster on the support surface, then the rate of dissociation of CO could be readily enhanced relative to what was observed in solution. One other possibility is that the structure on the silica surface that has lost a CO ligand is more flexible than that still having the CO bound, leading to a higher entropy in the products than in the reactant because of the constraints imposed by the surface. In solution, this constraint would be less likely, as shown by our SCRF calculations whereby the structures are more flexible and remain similar after CO loss.

It is clear that the chemistry is subtle and that there is much more to learn about support effects such as those indicated by the results presented here. These results appear to open a door broadly to control bonding and catalysis via support effects in metal complexes and metal clusters incorporating organic ligands. Thus, we infer design opportunities for metal complex and metal cluster catalysts that are not accessible by variation of organic solvents but are facilitated by controlled interactions between a support such as a metal oxide and a metal-containing active site.

Conclusions

Hydrogen activation on a trisubstituted tetrairidium carbonyl cluster was investigated both with the clusters dispersed on a dehydroxylated silica support and with the clusters dissolved in an inert solvent, *n*-decane. The same initial rates of CO loss from the silica-supported clusters at 323 K were observed for reaction in the presence of H_2 and, alternatively, helium, implying that the rate-determining step for hydrogen activation on the silica-supported clusters was CO dissociation. In contrast, for clusters dissolved in *n*-decane, the rate-determining step was different, involving an associative mechanism and both H_2 and CO ligands. When the reactions were investigated in the presence of helium, the CO dissociation rates were an order of magnitude higher for the silica-supported than for the dissolved clusters. These results demonstrate a novel control of chemistry on supported metal sites that are protected by organic ligands.

Conflicts of interest

There are no conflicts to declare.

Experimental

Materials and Sample Preparation

Details of the synthesis of $Ir_4L_3(CO)_9$ are reported elsewhere.[9] The clusters were adsorbed on dehydroxylated fumed silica (Degussa Aerosil 200, surface area 190 m^2/g) at room temperature from a slurry in *n*-hexane (EMD Chemicals, 95%). To clean the silica prior to use and synthesize a partially dehydroxylated surface, the silica was initially hydroxylated by refluxing in deionized water overnight. The silica-water mixture was cooled to room temperature and centrifuged (Thermofisher, Sorvall RC6) to separate the solid from the supernatant solution. The silica was then dried under vacuum at 473 K for 15 h and ground into a fine powder. Calcination was carried out at 723 K (temperature ramp, 5 K / min) in dry air for 4 h followed by 10 h of exposure to flowing helium. The BET surface area of the calcined silica was 190 ± 3 m^2/g.

n-Hexane was distilled and dried over sodium hydride prior to dissolution of the iridium clusters. The clusters were supported on the silica from a slurry in *n*-hexane using Schlenk-line techniques. Upon contact with the support, the solution containing the clusters quickly changed color from yellow to colorless, indicating that the clusters were transferred from solution to the silica. The slurry was stirred for one hour, and then the solvent was removed by evacuation at room temperature, so that all the

iridium remained on the support. The resultant solid sample contained 1.0 wt.% Ir. Reported results show that clusters remained intact after adsorption.[9] Samples were stored in an argon-filled glovebox (O_2 and H_2O monitor readings each < 5 ppm). All samples were handled using air-exclusion techniques.

Mass Spectrometry

An online Balzers OmniStar mass spectrometer running in multi-ion monitoring mode was used to record mass spectra of effluent gases from the flow reactor containing the supported iridium clusters. Prior to installation of the reactor in the flow system, helium was allowed to flow through the system for an hour to purge the lines of moisture and any other contaminants. Then the reactor was installed, and the temperature was ramped to 323 K at a rate of 3 K min^{-1}. Signals for H_2 (m/z = 2) and H_2O (m/z = 18) were monitored as O_2 flowed.

IR Spectroscopy

A Nicolet 6700 FTIR spectrometer with a spectral resolution of 2 cm^{-1} was used to collect transmission IR spectra of the supported samples. Approximately 30 mg of sample, containing 1.0 wt% Ir, was pressed into a wafer in the argon-filled glovebox and loaded into a cell that serves as a flow reactor (In-situ Research institute, Inc., South Bend, IN). The cell was sealed and promptly connected to the flow system to prevent exposure of the sample to air. All lines were purged with helium (Praxair, 99.999%) and, when the experiment involved flowing H_2, with H_2 (Praxair, 99.999%). Spectra characterizing recarbonylation were recorded as CO (Praxair, 99.999%) flowed through the system.

IR spectra of soluble clusters were recorded with samples in anhydrous *n*-decane solvent, chosen for its inertness and low volatility. Liquid samples were characterized with a Bruker Tensor 27 instrument with a spectral resolution of 2 cm^{-1} and a cell equipped with CaF_2 windows.

^{31}P CP/MAS NMR Spectroscopy

^{31}P solid-state CP/MAS NMR (CP contact time of 2 ms at 14 kHz sample spinning) spectra were measured using a Bruker Avance 500 MHz spectrometer with a wide bore 11.7 T magnet and employing a Bruker 4 mm MAS probe, at the Caltech Solid-State NMR Facility. The spectral frequencies were 500.23 MHz for the ^{1}H nucleus, and 202.5 MHz for the ^{31}P nucleus.

Decarbonylation Kinetics

Figures S14 and S15 in the ESI demonstrate the time scales used to determine the initial rates of decarbonylation of the supported samples in the presence of flowing helium and in the presence of flowing H_2. Initial rates were defined by establishing a characteristic time scale from decreasing terminal and bridging CO band intensities characterizing the clusters at 2043 and 1994 cm^{-1} and the bridging band at 1776 cm^{-1}; further details are shown in Table S1, ESI. It was assumed that no carbonyl ligands were removed from the clusters as they became linked to the supports, on the basis of previous work demonstrating an identical ratio of terminal to bridging carbonyl band areas characterizing $Ir_4L_3(CO)_9$ clusters dissolved in *n*-decane and those supported on SiO_2.[9] Data in Figures S6 and S9 (ESI) represent the number of (a) terminal and (b) bridging carbonyl ligands bound to the tetrahedral iridium framework. After establishing the time frame for determining the initial rate, the terminal and bridging carbonyl band areas were found for this time frame.

Computational Methods

Details of the computational methods are given in the ESI.

Acknowledgements

This work was supported by the U.S. Department of Energy (DOE), Office of Science, Basic Energy Sciences (BES), under Awards DE-FG02-04ER15513 (AP, BCG) and DE-FGO2-05ER15696 (AK). The NMR facility at the California Institute of Technology was supported by the National Science Foundation (NSF) under Grant Number 9724240 and partially supported by the MRSEC Program of the NSF under Award Number DMR-520565. This work was also supported in part by the DOE Office of Science, BES, under the DOE BES Catalysis Center Program by a subcontract from Pacific Northwest National Laboratory (KC0301050-47319). DAD also thanks the Robert Ramsay Chair Fund of The University of Alabama for support.

Keywords: iridium cluster• hydride • tetrairidium • hydrogen activation

1 T. Bein, S. J. McLain, D. R. Corbin, R. D. Farlee, K. Moller, G. D. Stucky, G. Woolery and D. Sayers, *J. Am. Chem. Soc.*, 1988, **110**, 1801–1810.
2 Y. Lin and R. G. Finke, *J. Am. Chem. Soc.*, 1994, **116**, 8335–8353.
3 S. Bordiga, G. Turnes Palomino, D. Arduino, C. Lamberti, A. Zecchina and C. Otero Areán, *J. Mol. Catal. A Chem.*, 1999, **146**, 97–106.
4 J. Saavedra, H. A. Doan, C. J. Pursell and C. Lars, *Science*, 2014, **345**, 1599–1602.
5 B. C. Gates, M. Flytzani-Stephanopoulos, D. A. Dixon and A. Katz, *Catal. Sci. Technol.*, 2017, **7**, 4259–4275.
6 P. Basu, D. Panayotov and J. T. Yates, *J. Am. Chem. Soc.*, 1988, **110**, 2074–2081.
7 N. De Silva, J. Ha, A. Solovyov, M. M. Nigra, I. Ogino, S. W. Yeh, K. A. Durkin and A. Katz, *Nat. Chem.*, 2010, **2**, 1062–1068.
8 M. Behrens, F. Studt, I. Kasatkin, S. Kuhl, M. Havecker, F. Abild-Pedersen, S. Zander, F. Girgsdies, P. Kurr, B.-L. Kniep, M. Tovar, R. W. Fischer, J. K. Nørskov and R. Schlogl, *Science*, 2012, **336**, 893–897.
9 A. Palermo, A. Solovyov, D. Ertler, A. Okrut and B. C. Gates, *Chem. Sci.*, 2017, **8**, 4951–4960.
10 L. M. Bavaro, P. Montangero and J. B. Keister, *J. Am. Chem. Soc.*, 1983, **105**, 4977–4981.
11 F. J. Safarowic, D. J. Bierdeman and J. B. Keister, *J. Am. Chem. Soc.*, 1996, **3**, 11805–11812.
12 A. Okrut, R. C. Runnebaum, X. Ouyang, J. Lu, C. Aydin, S.-J. Hwang, S. Zhang, O. A. Olatunji-Ojo, K. A. Durkin, D. A. Dixon, B. C. Gates and A. Katz, *Nat. Nanotechnol.*, 2014, **9**, 459–465.
13 A. Okrut, O. Gazit, N. De Silva, R. Nichiporuk, A. Solovyov and A. Katz, *Dalt. Trans.*, 2012, **41**, 2091.
14 M. Chen, J. E. Dyer, B. C. Gates, A. Katz and D. A. Dixon, *Mol. Phys.*, 2012, **110:15**-**16**.
15 R. Psaro, C. Dossi, A. Fusi, R. Della Pergola, L. Garlaschelli, D. Roberto, L. Sordelli, R. Ugo and R. Zanoni, *J. Chem. Soc., Faraday Trans*., 1992, **88**, 369–376.
16 S. Kawi, J.-R. Chang and B. C. Gates, *J. Phys. Chem.*, 1993, **97**, 5375–5383.
17 D. C. Sonnenberger and J. D. Atwood, *J. Am. Chem. Soc.*, 1982, **104**, 2113–2116.
18 J. P. Collman, *J. Am. Chem. Soc.*, 1968, **1**, 136–143.
19 L. Vaska and J. W. DiLuzio, *J. Am. Chem. Soc.*, 1962, **84**, 679–680.
20 F. Correa, R. Nakamura, R. E. Stimson, R. L. Burwell and D. F. Shriver, *J. Am. Chem. Soc.*, 1980, **102**, 5112–5114.
21 J.-M. Ha, A. Soloyyov and A. Katz, *J. Phys. Chem. C*, 2010, **114**, 16060–16070.
22 J.-M. Ha, A. Solovyov and A. Katz, *Langmuir*, 2009, **25**, 10548–10553.
23 C. Schöttle, E. L. Clark, A. Harker, A. Solovyov, A. T. Bell and A. Katz, *Chem. Commun.*, 2017, **53**, 10870–10873.
24 M. J. Wax and R. G. Bergman, *J. Am. Chem. Soc.*, 1981, **103**, 7028–7030.
25 A. Tousignant and J. N. Pelletier, *Chem. Biol.*, 2004, **11**, 1037–1042.

Journal

ARTICLE